nature cell biology

Wurst is essential for airway clearance and respiratory-tube size control

Matthias Behr[1], Christian Wingen[1], Christian Wolf[2,3], Reinhard Schuh[2] and Michael Hoch[1,4]

The *Drosophila melanogaster* tracheal system and the mammalian lung are branching networks of tubular epithelia that convert during late embryogenesis from liquid- to air-filling[1–3]. Little is known about how respiratory-tube size and physiology are coordinated. Here, we show that the *Drosophila wurst* gene encodes a unique J-domain transmembrane protein highly conserved in metazoa. In *wurst* mutants, respiratory-tube length is increased and lumen clearance is abolished, preventing gas filling of the airways. Wurst is essential for clathrin-mediated endocytosis[4], which is required for size determination and lumen clearance of the airways. wurst recruits heat shock cognate protein 70-4 and clathrin to the apical membrane of epithelial cells. The sequence conservation of the single Wurst orthologues in mice and humans offer new opportunities for genetic studies of clinically relevant lung syndromes caused by the failure of liquid clearance and respiratory-tube size control.

Many organs, including the lung, the kidney and the cardio-vascular system, transport fluids or gases through an intricate network of branched epithelial tubes or endothelial vessels[5,6]. During human lung development, dichotomously branching tubes of distinct length and diameter are generated, resulting in a complex tubular network that carries oxygen to the alveoli, where it diffuses into blood to be distributed to the tissues[7]. In the fruit fly *Drosophila melanogaster*, gas exchange is mediated by the tracheal system, which also consists of a network of branching epithelial tubes[1]. Both the fly tracheal system and the mammalian airways share many common features in development and function. Key molecular mechanisms of patterning and branching are mediated by conserved growth factors and signalling cascades in both systems[3,8]. During normal development of the airways, morphological and physiological processes, such as tube-size determination[9] and the transition from liquid- to air-filled tubes, occur during tube maturation in later stages of embryogenesis[1]. Defects in tube length and diameter strongly compromise the rate of gas exchange. The retention of liquid at birth impairs oxygenation of the blood, and severe fluid retention is an important feature of neonatal respiratory distress syndrome, the most common cause of death among premature and newborn infants[10]. Respiratory-tube regulators that are involved in the coordination of both tube morphology and physiology are, however, unknown.

In a search for genes controlling tube maturation in the *Drosophila* tracheal system, a P insertion was identified in a genetic locus that we named *wurst*. Hemizygous *wurst* mutants show an increased tracheal length and diameter resulting in curved tracheal branches (Fig. 1a, b). Molecular and genetic analysis indicate that the *wurst* P-element allele represents a strong hypomorphic allele and genetic rescue experiments demonstrate that the lethality of the P allele is linked to *wurst* gene function (see Supplementary Information, Fig. S1).

The *wurst* gene encodes a protein containing six putative transmembrane domains, a type 1 clathrin binding motif (C1; see Supplementary Information, Fig. S1) and a carboxy-terminal cytoplasmic J-domain (Fig. 1c, d). The J-domain is a conserved motif of cytoplasmic dnaJ proteins, which bind to members of the constitutively expressed heat shock cognate protein (hsc70) family as cochaperones and stimulate their low intrinsic ATPase activity[11–14]. Single-copy genes of putative *wurst* orthologues are found in invertebrates and in mammals (Fig. 1e). The transmembrane domains, the C1 motif and the J-domains of the wurst orthologues are highly conserved (Fig. 1d), indicating that wurst represents the prototype of a novel class of conserved J-domain transmembrane proteins.

Phenotypic analysis demonstrates that the *wurst* tube-length phenotype is caused by defective extracellular matrix (ECM) organization in the tracheal tubes (Fig. 2a–h). In wild-type embryos, chitin and associated binding proteins are secreted into the lumen of the respiratory tubes from stage 13 onwards, to establish a central chitin cable and a surrounding gap region that is devoid of chitin (Fig. 2a). It has been shown that septate-junctions proteins[15,16] or chitin-modifying enzymes are crucial for the establishment of proper ECM organization and tracheal-tube size. At stage 17 of embryogenesis, the chitinous ECM is degraded and lumen clearance occurs to enable gas filling of the respiratory

[1]LIMES-Institute, Program Unit Development & Genetics, Laboratory for Molecular Developmental Biology, University of Bonn, Meckenheimer Allee 169, D-53115 Bonn, Germany. [2]Max-Planck-Institute for Biophysical Chemistry, Molecular Developmental Biology, Am Fassberg 11, D-37077 Göttingen, Germany. [3]Current address: Intervet Innovation GmbH, Drug Discovery / Target Discovery, Zur Propstei, D-55270 Schwabenheim, Germany.
[4]Correspondence should be addressed to M.H. (e-mail: m.hoch@uni-bonn.de)

Received 3 May 2007; accepted 24 May 2007; published online 10 June 2007; DOI: 10.1038/ncb1611

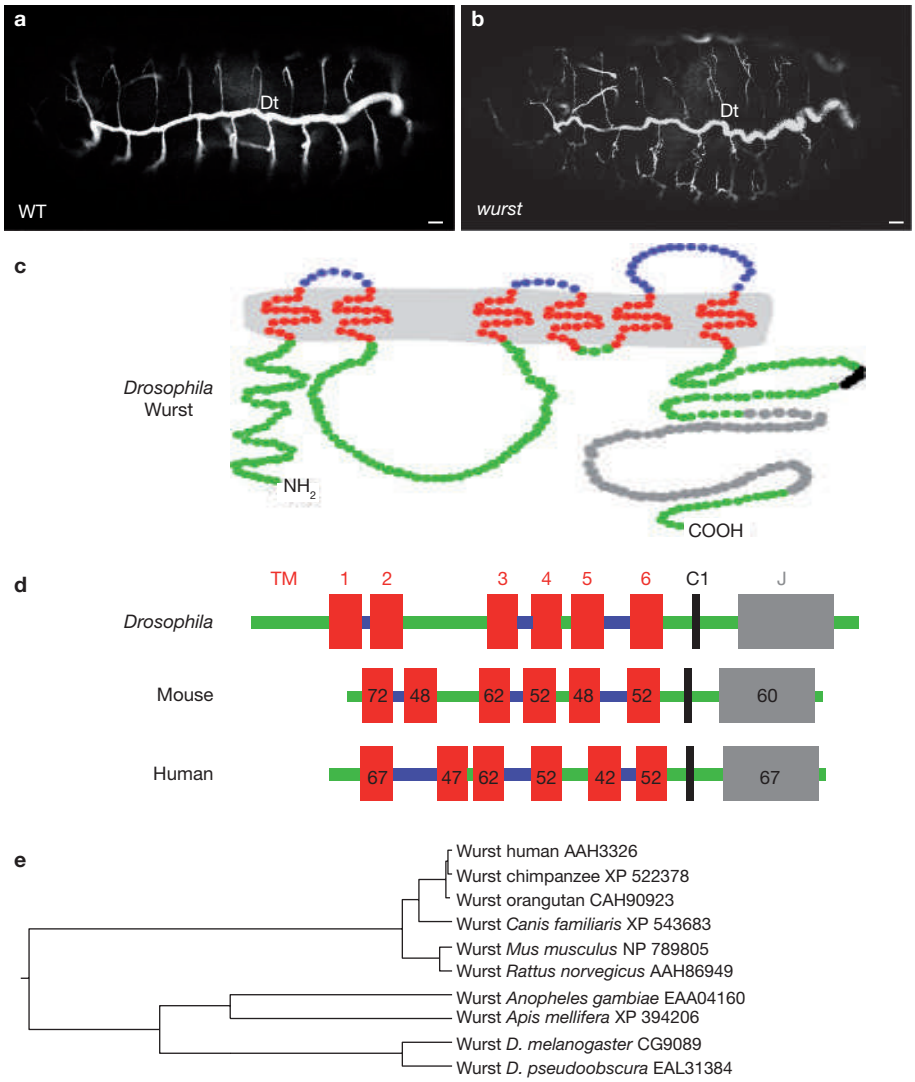

Figure 1 Wurst is a conserved protein required for respiratory-tube size control. (**a**, **b**) Antibody stainings using 2A12 as a tracheal lumen marker in embryos at early stage (st) 16 reveal elongated tube length in *wurst* mutants compared to wild type (WT). Dt, dorsal trunk. (**c**, **d**) Schematic representation of the predicted domain structure of wurst (**c**) and its orthologues (**d**). They contain six transmembrane (TM)-domains (red), a putative clathrin binding motif (C1; black) and a highly conserved J-domain (grey). Numbers indicate percentage sequence similarity. (**e**) Phylogenetic tree of wurst orthologues. The scale bars represent 10 μm in **a** and **b**.

tubes shortly before the larva hatches[17]. Although the secretion of the ECM into the lumen of the respiratory tubes occurs normally in *wurst* mutants, its organization into the central chitin cylinder and the gap region fails to occur, as visualized using the chitin markers wheat-germ agglutinin (wga) and chitin-binding protein (cbp; Fig. 2b). Consistently, chitin modifying enzymes, such as the putative polysaccharide deacetylase serpentine (serp)[19] or knickkopf (knk)[20,21], are secreted normally into the lumen of *wurst* mutant tubes, but fail to be localized properly (Fig. 2c, d and data not shown). Electron microscopy studies further confirmed the disorganization of the chininous ECM and demonstrated an accumulation of chitin fibres in the tube lumens of *wurst* mutants (Fig. 2e, f). In contrast with wild type, in which the chitinous ECM is degraded and protein and liquid are removed from the tube lumens during embryonic stages 16 and 17 to enable gas filling, lumen clearance was absent in *wurst* mutants. Instead, chitin binding proteins (such as serp and wga) and tracheal lumen markers (such as 2A12) persisted in *wurst* mutants until the end of embryogenesis, instead of being cleared as in wild type (Fig. 2i, j and see Supplementary Information, Fig. S1). The failure of lumen clearing was confirmed by electron microscopy studies (Fig. 2e–h). As a consequence, gas filling fails to occur in *wurst* mutant embryos (Fig. 2k, l), which die as late embryos.

To study the molecular function of wurst, an anti-wurst antibody was generated. Wurst, which has a maternal component, begins to be zygotically expressed from embryonic stage 13 onwards in all epithelial tissues, including the developing tracheal tubes (see Supplementary Information, Fig. S1). Biochemical fractionation assays and confocal microscopy indicated that wurst protein is localized at distinct sites in the plasma membrane and extensively in cytoplasmic vesicles (see Supplementary Information, Figs S1, 2). Coimmunostaining of wurst with endosomal markers such as rab5 (ref. 22) showed partial colocalization, indicating that wurst is contained within early endosomal compartments (see Supplementary Information, Fig. S2).

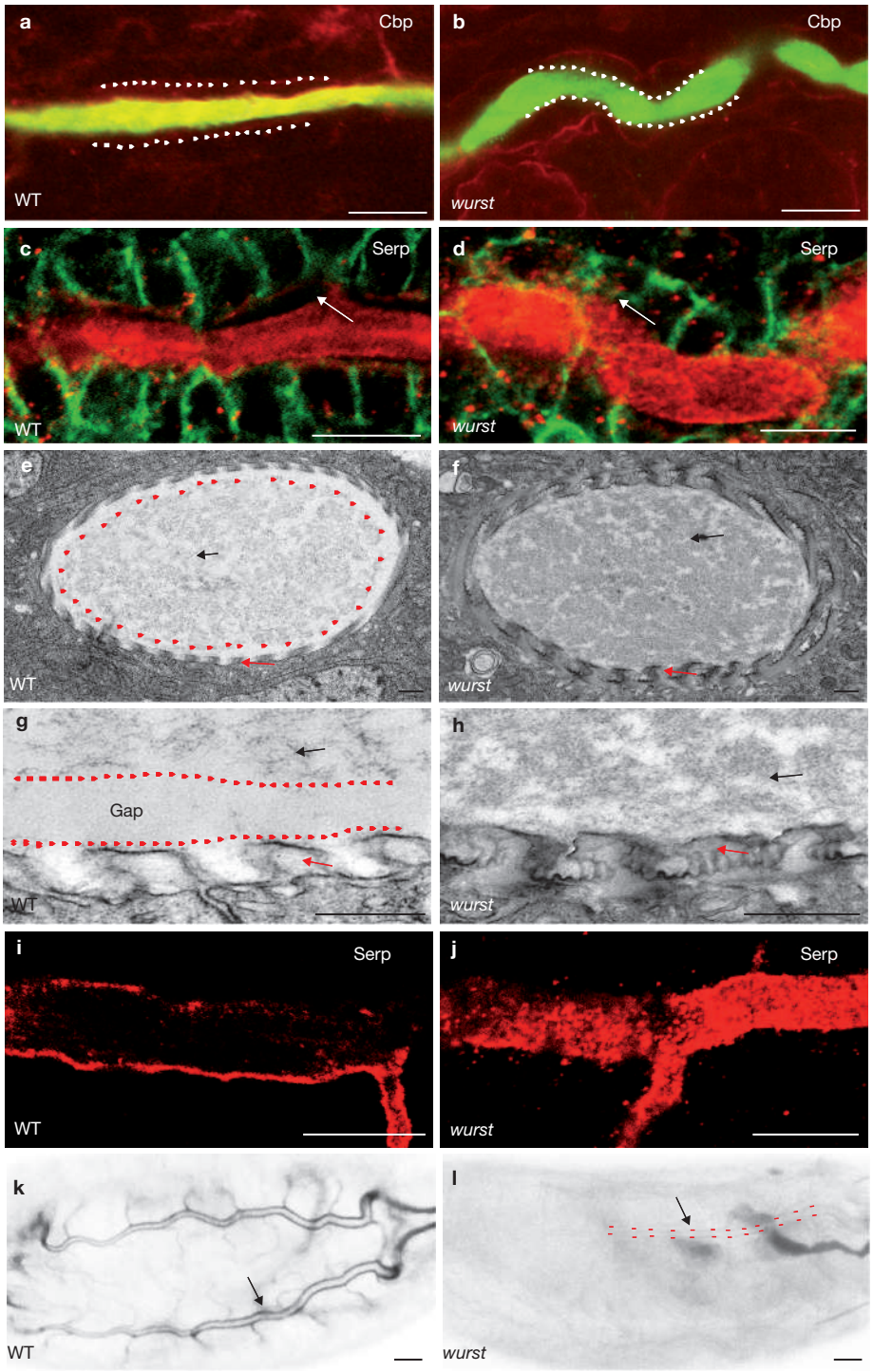

Figure 2 Wurst is required for apical ECM organization and respiratory lumen clearance. (**a**, **b**) In wild-type cells (**a**), immunostaining of the chitin-binding protein (cbp, green; wga, red) marks the central chitin cylinder; the gap region inbetween the central cylinder and the apical tracheal-cell membranes (white dots) remains chitin-free. In *wurst* mutants (**b**), the chitinous ECM is disorganized, the gap region is lost, and cbp and chitin are evenly distributed over the entire lumen reaching towards the apical membrane (white dots). (**c**, **d**) ECM proteins such as serp (red; α-spectrin as a membrane marker in green) are restricted to the inner-tube cylinder in wild-type cells leaving a gap region towards the apical membrane (arrow), but are mislocalized over the entire tube lumen in *wurst* mutants. A gap region is not detectable (arrow). (**e**–**h**) Electron microscopy studies confirm the loss of the gap region in *wurst* mutants and a disorganization of the chitin fibres (black arrows; taenidial folds are indicated by red arrows and the gap region by red dots). (**i**, **j**) In late stage 17 embryos, serp and other ECM components are cleaned from the inner-cylinder lumens to allow gas filling. Lumen clearance fails to occur in *wurst* mutants. (**k**, **l**) In wild-type embryos, gas filling can be observed due to the change of light refraction (arrows). Gas filling fails in *wurst* mutants (red dots mark a tracheal tube). The scale bars represent 500 nm in **e**–**h**, and 10 μm in **a**–**d** and **i**–**l**.

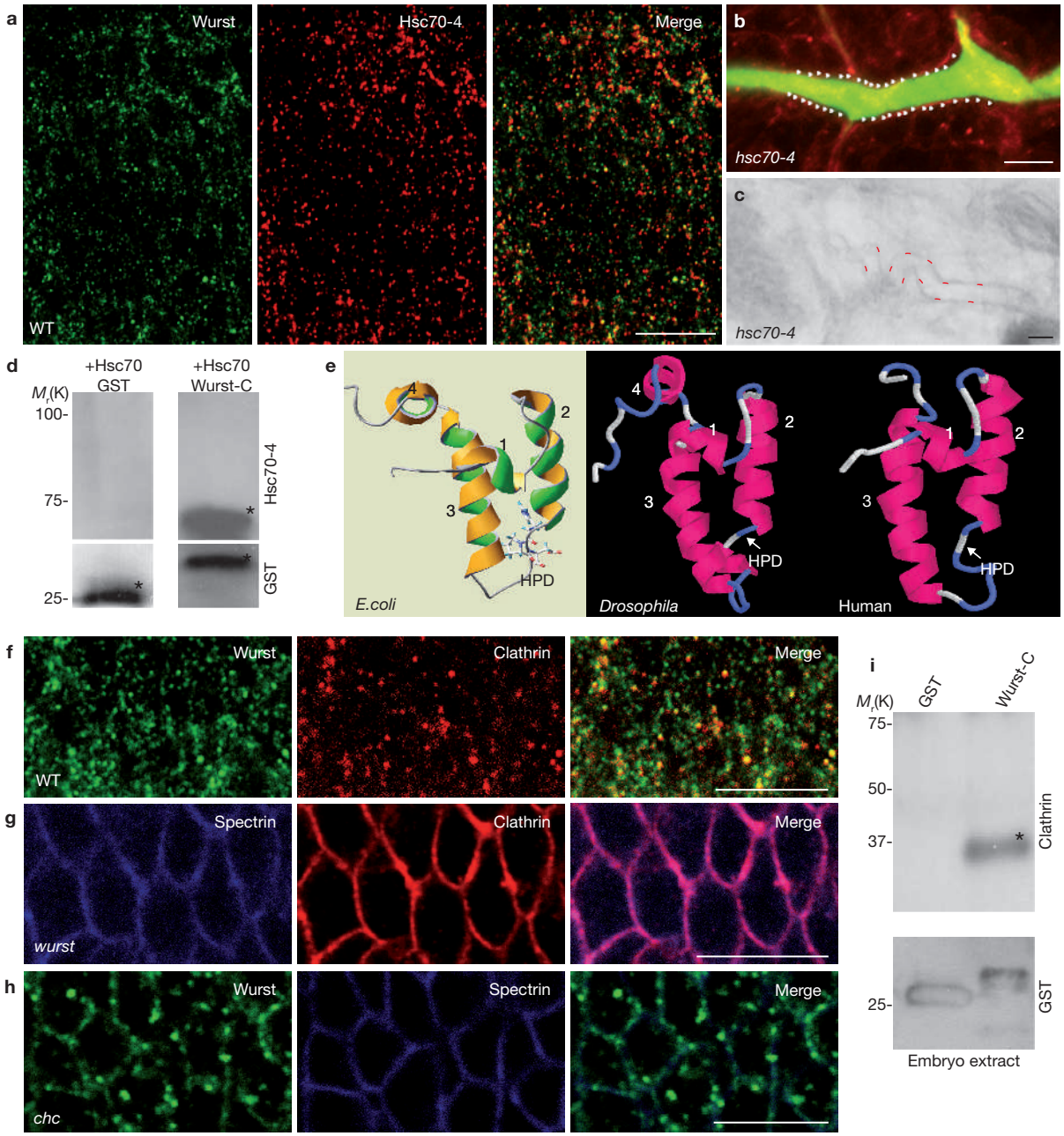

Figure 3 Wurst interacts with hsc70-4 and clathrin. (**a**) Immunostaining of embryonic epidermal cells reveal colocalization of wurst (green) with hsc70-4 (red). (**b**, **c**) Embryos in which dominant-negative hsc70-4 is expressed in the tracheal cells (driver line btlG4) show a disorganized chitinous ECM, as visualized by cbp expression (**b**) and a failure of gas filling (**c**). (**d**) Interaction *in vitro*. The wurst C-terminus (containing the J-domain) fused to GST (asterisks) directly interacts with hsc70-4 (see Supplementary Information, Fig. S5). (**e**) Schematic representation of highly similar structures of the J-domains of the *E. coli* DnaJ protein[14] and *Drosophila* and human wurst predicted by computational modelling. (**f**) Coimmunostaining of wurst (green) and clathrin (red) in stage 16 wild-type epidermal cells. Both proteins partially colocalize. (**g**) In stage 16 *wurst* mutants, clathrin (red) accumulates at the plasma membrane and colocalizes with the membrane marker α-spectrin (blue). (**h**) In stage 16 *clathrin* (*chc*) mutants, wurst (green) accumulates at the plasma membrane of epidermal cells and shows extensive colocalization with α-spectrin (blue). (**i**) Clathrin light chain is specifically pulled down (see asterisk) from embryonic extracts by the wurst C-terminus fused with GST, which includes the putative clathrin-binding motif (see Supplementary Information, Fig. S5). The scale bars represent 10 μm in all panels.

The conserved J-domain of wurst suggests that it may interact with members of the hsc70 family. In *Drosophila* embryos, two subtypes of hsc70 are predominantly expressed[23]: hsc70-3 (or bip), which is associated with the luminal endoplasmic reticulum, and hsc70-4. Hsc70-4 has been implicated in the uncoating of clathrin from clathrin-coated vesicles (CCV). *In vitro* evidence suggests that it can bind to dynamin[24] and may also have a role in the early steps of CCV formation[25–27]. Consistently, expression of dominant-negative form of hsc70-4 or *hsc70* mutants[25] were shown to cause defects in clathrin-dependent internalization and in receptor recycling. Although hsc70-3 and wurst did not colocalize (see Supplementary Information, Fig. S2), wurst did colocalize with hsc70-4 in embryonic ectodermal cells (Fig. 3a). Furthermore, expression of a

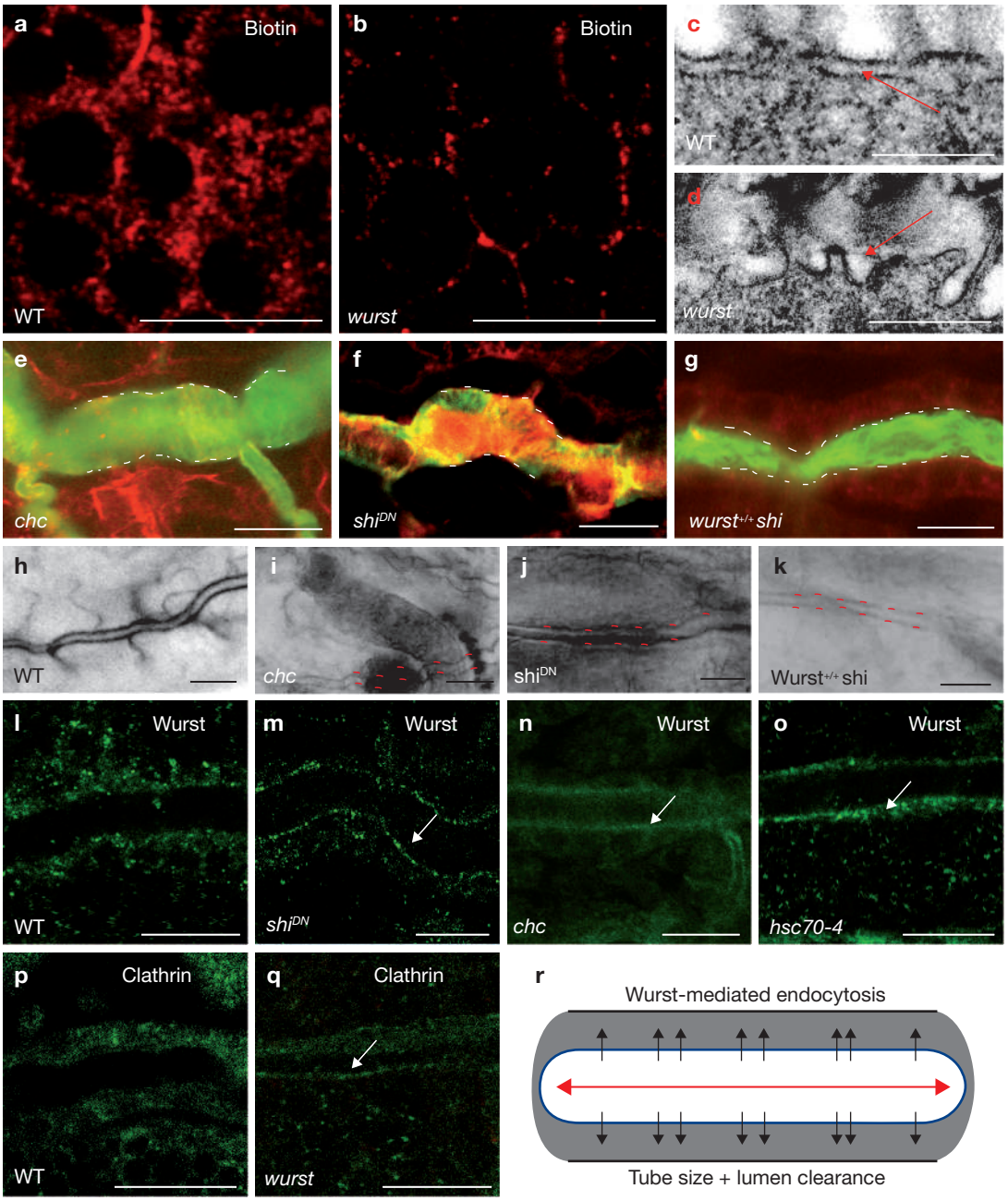

Figure 4 Wurst-dependent endocytosis is essential for tube-size regulation and lumen clearance. (**a**, **b**) Biotin tracer internalization is reduced in *wurst* mutants compared to wild-type epidermal cells, indicating defective endocytosis. (**c**, **d**) Electron microscopy studies reveal that in contrast to wild type, the apical cell membranes (arrows) of tracheal cells are enlarged in *wurst* mutants. (**e**–**g**) Immunostainings using cbp (green) and wga in red) reveal that the chitinous ECM is disorganized and the gap region is lost (white dots indicate apical membrane) in *clathrin* (**e**; *chc)*, *dynamin* (**f**; UAS–shi^{DN} misexpressed in tracheal cells) and in transheterozygous $wurst^{+/+}$ shi^{ts1} embryos (**g**) at the restrictive temperature; the same transheterozygous genotype at permissive temperature was used as control and showed no phenotype. (**h**–**k**) Gas-filling phenotypes of endocytosis mutants. (**l**–**o**) In stage 16 embryos in which the dominant-negative version of dynamin (UAS–shi^{DN}) was misexpressed (**m**), wurst accumulates at the apical plasma membrane (arrow) of tracheal tubes, as it is the case in *chc* (**n**) and *hsc70-4* (**o**) mutants. (**p**, **q**) Clathrin accumulates in *wurst*-mutant embryos at the apical plasma membrane of tracheal cells compared to wild type. (**r**) Schematic representation of wurst-mediated endocytosis and its role in tube maturation. Tube size is indicated by the red arrow and lumen clearance by black arrows. The scale bars represent 10 μm in **a**, **b** and **e**–**q**, and 200 nm in **c** and **d**.

dominant-negative form of *hsc70-4* in tracheal cells caused disorganization of the chitin ECM (Fig. 3b), defective lumen clearance and a strong reduction in gas filling (Fig. 3c), as observed in *wurst* mutants (Fig. 2b, l). In contrast, *hsc70-3* mutants showed no phenotype in chitin ECM organization. Coimmunoprecipitation assays with the wurst C-terminus containing the J-domain and hsc70-4 demonstrated that both proteins interact directly (Fig. 3d and see Supplementary Information, Fig. S1). This was consistent with computational modelling of the *Drosophila* and human wurst J-domains (Fig. 3e). Both show extensive structural similarity to the J-domain of the *Escherichia coli* DnaJ protein, which is known to bind to the hsc70 homologue DnaK and function as a cochaperone. The structure of the *E. coli* J-domain has been solved, and

was shown to contain 4 α-helices and an essential HPD binding motif between the second and third helix[14]. These hallmarks of the J-domain structure are conserved in wurst J-domains, suggesting that wurst orthologues of other species may also interact with hsc70.

As wurst contains a putative clathrin-binding motif, we also biochemically and genetically tested whether wurst interacts with clathrin. Coimmunostaining showed that wurst and clathrin were colocalized in both S2 tissue culture cells and in embryonic ectodermal cells (Fig. 3f and see Supplementary Information, Fig. S2). In contrast to wild type, in which clathrin was distributed in a punctate pattern at the plasma membrane and the cortical cytoplasm of epithelial cells, clathrin accumulated at the membrane of *wurst* mutant cells (Figs 3g and 4q). Similarly, wurst accumulated at the membrane of *clathrin heavy chain* (*chc*) mutant cells (Figs 3h and 4n), indicating that the proper localization of the both proteins is mutually dependent on each other. Consistently, we found a physical interaction of clathrin and wurst in pulldown assays using embryonic extracts (Fig. 3i).

A role for wurst in endocytosis was further tested by using tracer-uptake assays[25]. A reduction in endocytosis was found in *wurst* mutants and on RNA interference (RNAi) knockdown of *wurst* in S2 cells (Fig. 4a, b and see Supplementary Information, Fig. S4) indicating an important role of *wurst* in endocytotic processes. Electron microscopy studies show that the apical membrane of *wurst* mutant tracheal cells is disorganized and contains folds that are likely to be due to extra-membrane material, as compared to wild-type cells (Fig. 4c, d). To further determine whether key regulators of endocytosis are involved in respiratory-tube size determination and lumen clearance in the *Drosophila* airways, *clathrin* and *dynamin* (*shibire*) mutants were analysed. *chc* mutants showed a *wurst*-like mutant phenotype, with an extension of tracheal-tube length, a failure of luminal chitin ECM organization (Fig. 4e) and a loss of lumen clearance, resulting in defective gas filling (Fig. 4i). A similar mutant phenotype was induced in *dynamin* mutants ($shibire^{DN}$ or $shibire^{ts1}$; Fig. 4f, j) or in transheterozygous embryos carrying a single mutant allele of *wurst* and of $shibire^{ts1}$ (*wurst*,+/+, $shibire^{ts1}$; Fig. 4g, k). Consistently, wurst accumulated at the membrane in *shibire* and other endocytosis mutants (Fig. 4l–o), providing further evidence that wurst and dynamin function in a common pathway essential for respiratory-tube maturation.

Our results identify wurst as the first regulator that is essential for both tube-size determination and lumen clearance in the *Drosophila* airways (Fig. 4r). Furthermore, we have established that wurst-dependent endocytosis is critical for the maturation of the respiratory tubes. Wurst is ubiquitously expressed in embryonic epithelial cells; however, it is strongly upregulated when endocytosis-dependent lumen clearance has to occur during tracheal tube maturation. Unlike the other known cytoplasmic J-domain proteins auxilin and rme-8, which are also involved in clathrin-mediated endocytosis[4], wurst is a transmembrane protein localized in the plasma membrane. We propose that it recruits hsc70-4 and clathrin to the apical membrane and may thus coordinate the early steps of clathrin-mediated endocytosis, consistent with the accumulation of clathrin and the apical membrane enlargement in *wurst* mutants. When the clathrin coats are dissociated from CCVs and re-used for subsequent rounds of endocytosis, wurst is kept in vesicles that subsequently enter the endosomal pathway, and may have other unknown functions there. One protein family that may represent a cargo of wurst-mediated endocytosis are epithelial Na^+ channels (ENaCs), as indicated by genetic-interaction experiments (see Supplementary Information, Fig. S3). From the 16 ENaC genes in *Drosophila*, nine are expressed in the tracheal cells and knockdown of two family members has indicated that these proteins are involved in the regulation of liquid clearance[28], similarly to in the mammalian airways[29]. It is of note that mice and humans only contain a single wurst orthologue each, which is highly similar in sequence and structure to the *Drosophila* wurst. Preliminary data suggests that the single mouse and human *wurst* orthologues are expressed in the lung and other tubular epithelia (see Supplementary Information, Fig. S4). Our findings, and the extensive similarities between *Drosophila* and mammalian airways[3], may thus offer new opportunities for genetic studies to decipher the putative roles of wurst orthologues in clinically relevant lung syndromes, including neonatal respiratory distress syndrome caused by the failure of liquid clearance and defects in size determination of the airways. □

METHODS

Electron microscopy. Embryos were collected for 2 h then grown to stage 17 and genotyped for GFP expression. Embryos were embedded in 2% agarose and post fixed with 5% glutaraldehyde for 2 h at room temperature. Ultra-thin sections were prepared and analysed using a Zeiss Libra 120 electron microscope.

Endocytosis assays. Sulphur–NHS–biotin (#21217; Pierce, Rockford, IL) or FM4-64 (Molecular Probes, Eugene, OR) tracers, which are known to be taken up into apical and subapical compartments in a time-dependent manner, were used. Sulphur–biotin contains a unique spacer and is used for biotinylation of cell-surface proteins. FM4-64 inserts into the outer leaflet of the plasma membrane. Both markers do not enter cells only by diffusion. Ten-thirteen-day-old embryos were collected, genotyped for GFP expression, transferred to glass slides and mounted with glue from standard adhesive tape. Embryos were washed with PBS, cut and tracer was added. In most of the cut embryos used, the vitelline membrane was either largely lost, but still sticking enough to allow attachment to the glue of the cover slip, or the tracers diffused into the space inbetween the vitelline membrane and the epidermis, thereby reaching the apical surface of the cells. Only embryos were used for our analysis in which we were sure that the tracer reached only the apical side of the cells. After 2 min, free remaining tracer was washed off with PBS three times. For cellular tracer internalization, embryos were incubated additionally for 10 min at 22 °C, fixed with 4% formaldehyde (10 min) and washed with PBS. Sulphor–biotin was detected by an anti-Biotin primary antibody (1:200, mouse) and by a secondary Cy3-conjugated anti-mouse antibody (1:500, goat; JacksonImmuno, Newmarket, UK). Images were taken using a Leica TCS SP2 confocal system. Each fluorochrome was scanned individually to avoid crosstalk between channels. For S2 cells similar conditions were used: S2 cells were plated on a cover slide washed with PBS and treated with sulphur–biotin for 2 min, washed three times with PBS, and incubated for an additional 10 min for internalization. Afterwards, cells were fixed with 4% PFA. For antibody staining, cells were treated as described in the Supplementary Information, Methods.

Fly stocks. All stocks used are described at flybase (www.flybase.org). The $wurst^{l(1)G0162}$ line was a gift from U. Schäfer and H. Jäckle (Max-Planck Institute, Göttingen, Germany). UAS–*hsc4-K71* (dominant-negative mutant) was a gift from K. Palter (Temple University, Philadelphia, PA). UAS–*ppk11* was a gift from L. Liu (University of Iowa, Iowa City, IA). chc^1, shi^{ts1}, UAS–*shi-K44* (dominant-negative mutant) and balancers were obtained from the Bloomington *Drosophila* Stock Center (Bloomington, IN). Homozygous mutant embryos were genotyped for GFP expression (FM7i-actinGFP). The generation of transheterozygous mutants is described in detail in the Supplementary Information, Methods.

Immunostaining. Details of the immunostainings are described in the Supplementary Information, Methods. Anti-wurst antibodies were generated in guinea pig against the 14 C-terminal amino acids (RRKNKQYQEEEAIV) and affinity-purified by Eurogentec (Brussels, Belgium). The antibody was used at a 1:20 dilution for embryo whole-mount antibody staining and 1:300 for western blot analysis. Antibody staining and *in situ* hybridization were performed as previously described[15].

Immunoblotting, GST pulldowns and fractionation experiments. For glutathione–S-transferase (GST) experiments, the C-terminus (amino acids 271–406) of wurst was cloned into the pGEX-4T-3 vector. The GST–Wurst-C-terminus fusion protein was expressed at 22 °C for 30 min in *E. coli* cells. The fusion protein was purified with Sephadex 4B (Amersham, Piscataway, NJ; 1 h at 4 °C) and washed six times with ice-cold PBS buffer. For pulldown assays, the beads–GST–wurst-C-terminus complex was incubated with 0.5 μg Hsc70 bovine protein for 45 min at 4 °C and washed six times with ice-cold PBS buffer. Proteins were blotted for 1 h at 4 °C (Hybond protein^{+}) and the blot was cut below a relative molecular mass of 70,000 to detect Hsc70 (upper part) and GST (lower part). For protein detection, anti-Hsc70 (1:1000 western blot; 820, Stressgen, Victoria, Canada) and anti-GST (1:500, Amersham) were used as primary antibodies, and horseradish peroxidise-conjugated antibodies were used in combination with the chemiluminescence ECL system (Amersham) as secondary antibodies. To test for clathrin interaction, 10 μg embryo extract and anti-clathrin antibody (1:300; Sigma, St Louis, MO) was used. For GST detection, the blot was reused after stripping off antibody complexes.

Protein-structure analysis. Wurst protein-sequence analysis, structure prediction and domain modelling are described in the Supplementary Information. J-domain modelling was performed by using three-dimensional JIGSAW (http://www.bmm.icnet.uk/servers/3djigsaw/).

Tube-clearance assay. Embryos were collected for 2 h then grown to stage 17, dechorionated with 2.5% sodium hypochloride, transferred onto a glass slide, mounted with halocarbon oil and assayed at bright-field with an Olympus AX70 microscope.

Accession numbers. CG9089 (*Drosophila melanogaster*), AAH33236 (human), XP_522378 (chimpanzee), CAH90923 (orangutan), XP_543683 (*Canis familiaris*), NP_789805 (*Mus musculus*), AAH86949 (*Rattus norvegicus*), EAA04160 (*Anopheles gambiae*), XP_394206 (*Apis mellifera*) and EAL31384 (*Drosophila pseudoobscura*).

Note: Supplementary Information is available on the Nature Cell Biology website.

ACKNOWLEDGEMENTS

We thank: C. Samakovlis for communicating unpublished results; M. Affolter, R. Fehon, M. González-Gaitán, L. Liu, B. Moussian, K. Palter, D. F. Ready, U. Schäfer and S. Luschnig for sharing fly stocks and reagents; T. Magin, I. Zinke and B. Fuss for comments on the manuscript; and the members of the Hoch laboratory for helpful discussions. M.B. would like to thank L. Kutschenko, V. Arndt, J. Martini and all members of the Hoch laboratory for technical assistance. This work was supported by grants from the Deutsche Forschungsgemeinschaft (DFG) to M.B. (BE3215) and to M.H. (SFB 645).

AUTHOR CONTRIBUTIONS

Northern blot, electron microscopic studies and clathrin interaction assay were performed by C. Wingen; molecular analysis of the l(1)G0162 P-element was performed by C. Wolf; all other experiments were performed by M.B.; the wurst project was initiated by M.B. and R.S.; M.H. supervised the research project; M.H. wrote the manuscript; all authors discussed the experimental results.

COMPETING FINANCIAL INTERESTS

The authors declare no competing financial interests.

Published online at http://www.nature.com/naturecellbiology/
Reprints and permissions information is available online at http://npg.nature.com/reprintsandpermissions/

1. Manning, G. & Krasnow, M. in *The Development of Drosophila melanogaster.* (eds Bate,M. & Martinez Arias, A.) 609–685 (Cold Spring Harbor Laboratory Press, Cold Spring Harbor, 1993).
2. Olver, R. E., Walters, D. V. & M. Wilson, S. Developmental regulation of lung liquid transport. *Annu. Rev. Physiol.* **66,** 77–101 (2004).
3. Affolter, M. *et al.* Tube or not tube: remodeling epithelial tissues by branching morphogenesis. *Dev. Cell* **4,** 11–18 (2003).
4. Conner, S. D. & Schmid, S. L. Regulated portals of entry into the cell. *Nature* **422,** 37–44 (2003).
5. Hogan, B. L. M. & Kolodziej, P. A. Organogenesis: molecular mechanisms of tubulogenesis. *Nature Rev. Genet.* **3,** 513–523 (2002).
6. Davis, G. E. & Senger, D. R. Endothelial extracellular matrix: biosynthesis, remodeling, and functions during vascular morphogenesis and neovessel stabilization. *Circ. Res.* **97,** 1093–1107 (2005).
7. Fischer, H. & Widdicombe, J. H. Mechanisms of acid and base secretion by the airway epithelium. *J. Membr. Biol.* **211,** 139–150 (2006).
8. Metzger, R. J. & Krasnow, M. A. Genetic control of branching morphogenesis. *Science* **284,** 1635–1639 (1999).
9. Beitel, G. J.& Krasnow, M. A. Genetic control of epithelial tube size in the *Drosophila* tracheal system. *Development* **127,** 3271–3282 (2000).
10. O'Brodovich, H. M. Immature epithelial Na^{+} channel expression is one of the pathogenetic mechanisms leading to human neonatal respiratory distress syndrome. *Proc. Assoc. Am. Physicians* **108,** 345–355 (1996).
11. Ungewickell, E. *et al.* Role of auxilin in uncoating clathrin-coated vesicles. *Nature* **378,** 632–635 (1995).
12. Bukau, B., Weissman, J. & Horwich, A. Molecular chaperones and protein quality control. *Cell* **125,** 443–451 (2006).
13. Kelley, W. L. Molecular chaperones: How J domains turn on Hsp70s. *Curr. Biol.* **9,** R305–R308 (1999).
14. Pellecchia, M. *et al.* NMR structure of the J-domain and the Gly/Phe-rich region of the *Escherichia coli* DnaJ chaperone. *J. Mol. Biol.* **260,** 236–250 (1996).
15. Behr, M., Riedel, D. & Schuh, R. The claudin-like megatrachea is essential in septate junctions for the epithelial barrier function in *Drosophila. Dev. Cell* **5,** 611–620 (2003).
16. Wu, V. M. *et al.* Sinuous is a *Drosophila* claudin required for septate junction organization and epithelial tube size control. *J. Cell Biol.* **164,** 313–323 (2004).
17. Tonning, A. *et al.* A transient luminal chitinous matrix is required to model epithelial tube diameter in the *Drosophila* trachea. *Dev. Cell* **9,** 423–430 (2005).
18. Devine, W. P. *et al.* Requirement for chitin biosynthesis in epithelial tube morphogenesis. *Proc. Natl Acad. Sci. USA* **102,** 17014–17019 (2005).
19. Luschnig, S. *et al.* serpentine and vermiform encode matrix proteins with chitin binding and deacetylation domains that limit tracheal tube length in *Drosophila. Curr. Biol.* **16,** 186–194 (2006).
20. Wang, S. *et al.* Septate-junction-dependent luminal deposition of chitin deacetylases restricts tube elongation in the *Drosophila* trachea. *Curr. Biol.* **16,** 180–185 (2006).
21. Moussian, B. *et al. Drosophila* Knickkopf and Retroactive are needed for epithelial tube growth and cuticle differentiation through their specific requirement for chitin filament organization. *Development* **133,** 163–171 (2006).
22. Wucherpfennig, T., Wilsch-Brauninger, M. & Gonzalez-Gaitan, M. Role of *Drosophila* Rab5 during endosomal trafficking at the synapse and evoked neurotransmitter release. *J. Cell Biol.* **161,** 609–624 (2003).
23. Bronk, P. *et al. Drosophila* Hsc70-4 is critical for neurotransmitter exocytosis *in vivo*. *Neuron* **30,** 475–488 (2001).
24. Marks, B. *et al.* GTPase activity of dynamin and resulting conformation change are essential for endocytosis. *Nature* **410,** 231–235 (2001).
25. Chang, H. C. *et al.* Hsc70 is required for endocytosis and clathrin function in *Drosophila. J. Cell Biol.* **159,** 477–487 (2002).
26. Chang, H. C., Hull, M. & Mellman, I. The J-domain protein Rme-8 interacts with Hsc70 to control clathrin-dependent endocytosis in *Drosophila. J. Cell Biol.* **164,** 1055–1064 (2004).
27. Newmyer, S. L., Christensen, A. & Sever, S. Auxilin–dynamin interactions link the uncoating ATPase chaperone machinery with vesicle formation. *Dev. Cell* **4,** 929–940 (2003).
28. Liu, L., Johnson, W. A. & Welsh, M. J. *Drosophila* DEG/ENaC pickpocket genes are expressed in the tracheal system, where they may be involved in liquid clearance. *Proc. Natl Acad. Sci. USA* **100,** 2128–2133 (2003).
29. Hummler, E. *et al.* Early death due to defective neonatal lung liquid clearance in a-ENaC-deficient mice. *Nature Genetics* **12,** 325–328 (1996).

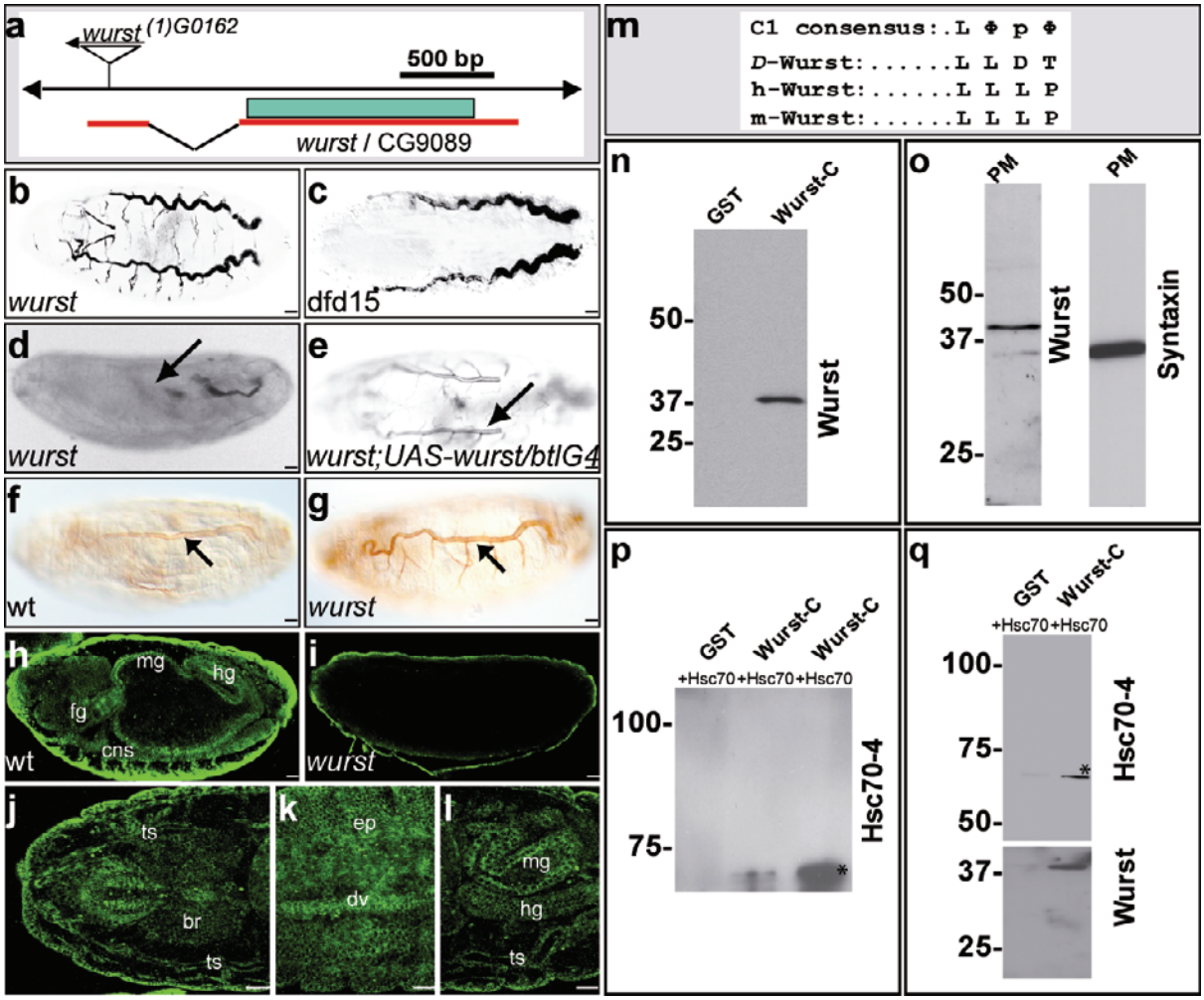

Figure S1 Molecular wurst analysis. **(a)** Molecular organization of the *wurst* transcription unit and the localization of the P-insertion. Exons are indicated in red and the ORF in green. **(b, c)** Hemizygous *wurst l(1)G0162* mutant embryos show a comparable tracheal size phenotype as the deficiency *dfd15* which deletes the *wurst* gene, indicating that the P allele is a strong hypomorphic or an amorphic allele. **(d, e)** Gas filling completely fails in *wurst* mutants (compare to Fig.1). Expressing UAS-wurst in *wurst* mutants with the tracheal driver line btlG4 rescued the gas filling phenotype to a large extent (arrows point to tracheal trunks). **(f, g)** Expression of the luminal marker 2A12 persists in the tracheal tubes of late st17 *wurst* mutant embryos, whereas it is cleared in wt embryos. Similarly, the zona pellucida protein Piopio, which is essential to interconnect the tracheal network, persists until st17 in tracheal tubes of *wurst* mutant embryos. **(h, j-l)** In wt embryos, wurst protein is expressed from st13 onwards within epithelial tissues, including the developing tracheal system (ts), the central nervous system (cns), the foregut (fg), the midgut (mg), the hindgut (hg), the brain (br), the epidermis (ep) and the dorsal vessel (dv). **(i)** wurst protein expression is strongly reduced or absent in *wurst* mutants, providing further evidence for the specificity of the anti-wurst antibody and indicating that the *wurst P* mutant is a strong hypomorphic or amorphic allele. **(m)** Clathrin binding consensus motif type 1 consists of a leucine and a sequence of amino acids with a hydrophobic (ϕ), polar (p), hydrophobic (ϕ) and negatively charged residue. This motif can be found in the *Drosophila*, human and mouse wurst C-termini. The negatively charged amino acid at the C-terminal end of the motif is not found in wurst proteins. **(n)** The anti-wurst antibody specifically detects the GST-wurst C-terminus fusion protein (see Methods) but not GST alone. **(o)** Biochemical fractionation of embryonic extracts to isolate the plasma membrane (PM) fraction; the anti-Wurst antibody detects a single polypeptide band of 46kDa in the PM fraction. The size of the polypeptide band corresponds to the predicted size of wurst. As a control the transmembrane protein syntaxin is detected in the same fraction. These data together with the predicted structure and the immunohistological analysis further support that wurst is a transmembrane protein. **(p, q)** Independent co-immunoprecipitation assays. The wurst C-terminus (containing the J-domain) fused to GST directly interacts with hsc70-4 (marked by asterisks; compare with Fig 3 d). Scale bar 10μm.

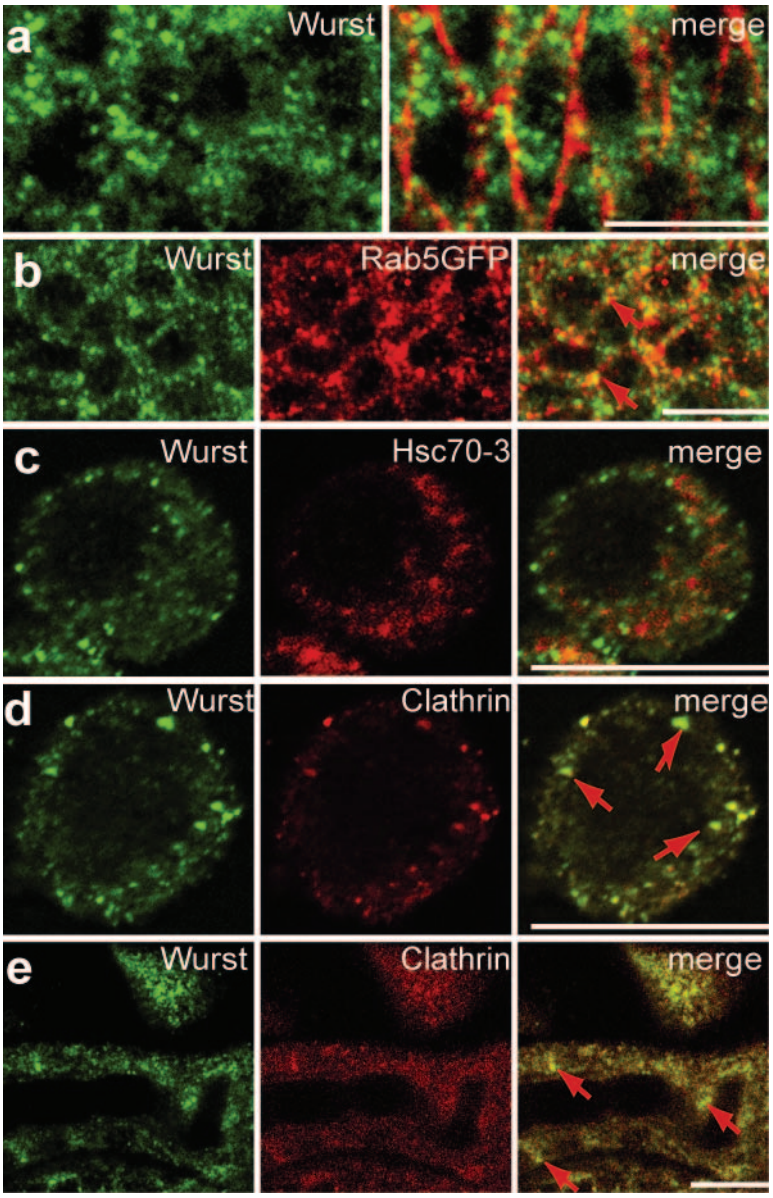

Figure S2 Wurst protein co-localization. **(a)** Co-localization study within epidermal cells of wurst (green) and the membrane marker alpha-spectrin (red) showing that wurst is localized at distinct sites in the plasma membrane and extensively in vesicles. **(b)** Wurst (green) can be observed in early endosomes as shown by co-localization (arrows) with Rab5GFP (red) in epidermal cells. **(c)** Immunostaining in S2 cells reveals that hsc70-3 (red) and wurst (green) are not co-localized. **(d, e)** Immunostaining in S2 cells (d) and embryonic tracheal cells (e) reveals co-localization (arrows) between wurst (green) and clathrin (red). Scale bar 10μm.

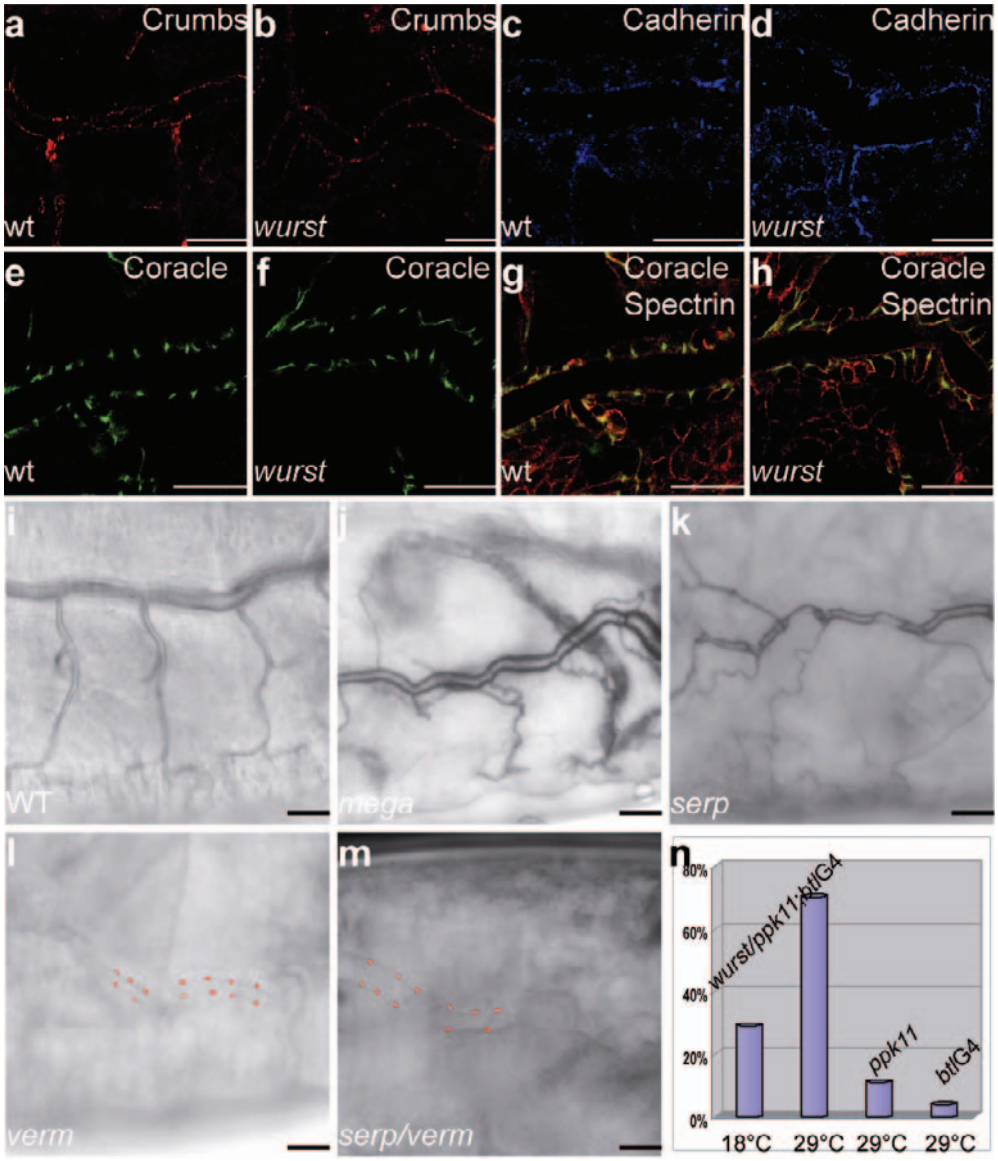

Figure S3 Cellular junction organization in wurst mutants and gas filling in mutants affecting tracheal tube size. Embryonic tracheal cells at st16. **(a, b)** Crumbs is part of the subapical region at the apicolateral cell membrane in wt cells (a); a mislocalization is not detectable in *wurst* mutant (b). **(b)** DE-cadherin is essential for adherens junctions, which are located at the apicolateral cell membrane in wt (c) and in *wurst* mutant cells (d). **(e-h)** Coracle (green) is an essential component of septate junctions, which are located at the lateral membrane and are necessary for barrier function and extracellular matrix secretion. Coracle localization in *wurst* mutants is similar to wt cells. Furthermore, co-localization studies with alpha-spectrin (red) show, that coracle localization does not expands basolaterally, as it is the case for other septate junction mutants. Injection experiments using the tracer Rhodamine labelled Dextran (MW 10,000; Molecular Probes) showed an intact barrier function indicating proper SJ function in *wurst* mutants (data not shown). **(i, j)** At late st 17 embryos gas filling takes place in wt **(i)** and *mega* mutant **(j)** embryos. Mega is essential to establish septate junctions, indicating that septate junctions are not necessary for gas filling. **(k-m)** We could observe partial gas filling in *serp* mutants (k) and no gas filling in *verm* (l) or *serp/verm* (m) double mutants (dotted lines indicate tracheal tubes). The reduction or failure of gas filling in these mutants is consistent with previous observations that the reduction of chitin deacytylation occurring in the mutants results in a failure of chitinous ECM degradation. **(n)** To explore whether ENaCs may represent a potential wurst cargo, *wurst* heterozygous mutants containing a single copy of a dominant negative UAS-*ppk11* allele were generated (driven by btlG4; for details see Methods below). ppk11 shows only a mild effect on gas filling (percentage of loss of gas filling is indicated by blue bars) but in *wurst* heterozygous mutant background, more than 70% of the embryos show no gas filling at 29°C (when Gal4 expression is strongest). At 18°C, when Gal4 expression is low, we observe less embryos with gas filling phenotypes (only about 30%). This genetic assay indicates that both, *wurst* and *ppk11* may act together to establish gas filling in embryos. Scale bar 10µm.

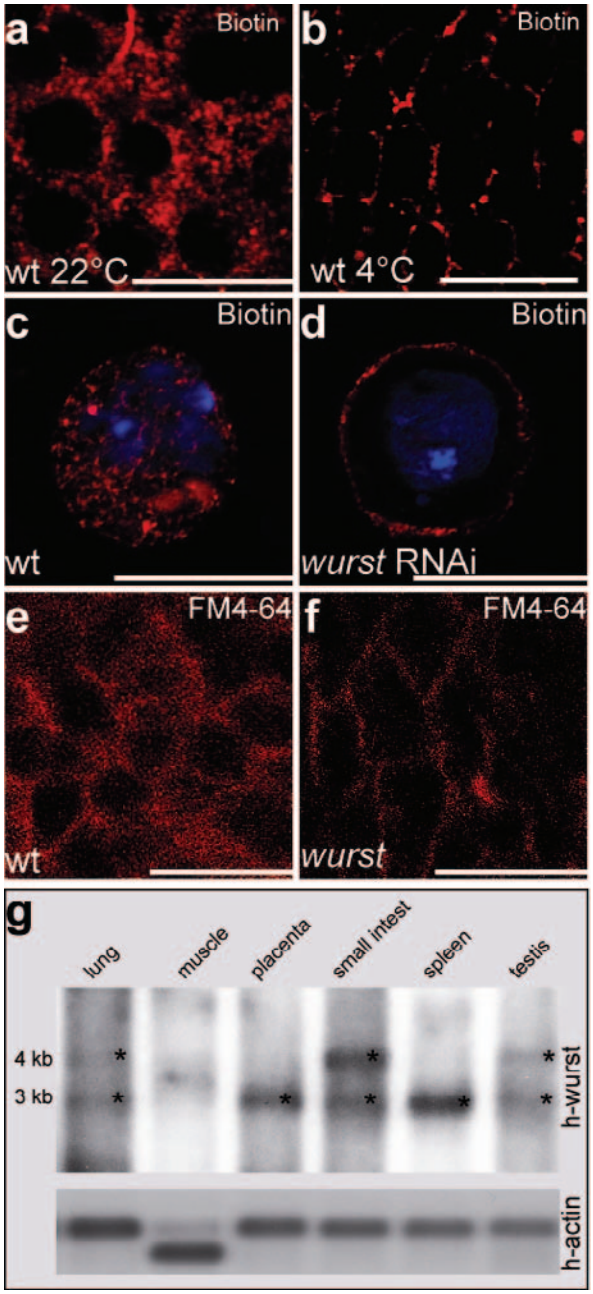

Figure S4 Endocytosis assay and human wurst expression. **(a, b)** In epidermal cells Biotin tracer internalisation is reduced at 4°C as compared to wt. **(c, d)** In WT S2 cells Biotin (red; DAPI in blue) tracer internalisation is detectable but not in *wurst* knock down cells, indicating defective endocytosis. **(e)** In comparison to WT epidermal cells FM4-64 internalization is reduced in *wurst* mutants. Scale bar 10µm. **(g)** Human *wurst* (*) is expressed in major epithelial tissues as shown by the upper Northern Blot analysis; the lower blot shows the human actin as a loading control. The murine wurst ortholog is also expressed in epithelial tissues, including lung and kidney (http://marvester.embl.de/marvester/Q8CH/Q8CHS2.htm). Scale bar 10µm.

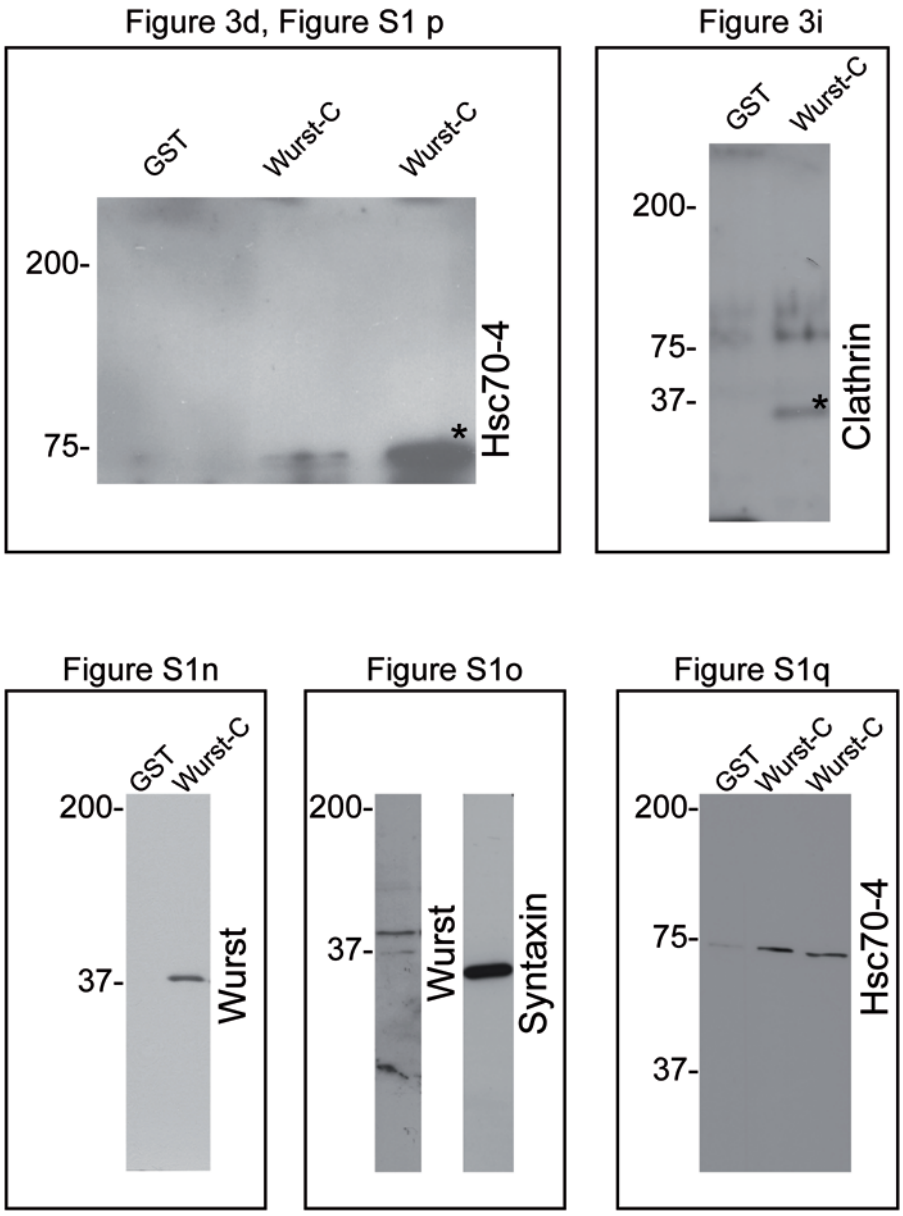

Figure S5: Full scans and panels of key Western data